

# Experimental and theoretical investigations of a low-pressure He–Xe discharge for lighting purpose

R. Bussiahn, S. Gortchakov, H. Lange, and D. Uhrlandt<sup>a)</sup>

*Institut für Niedertemperatur-Plasmaphysik Greifswald, Fr.-L.-Jahn-Str. 19, Greifswald 17489, Germany*

(Received 29 December 2003; accepted 22 February 2004)

Low-pressure cylindrical dc glow discharges in a mixture of helium and 2% xenon are studied by experiment and self-consistent modeling. They can be used for the design of mercury-free vacuum ultraviolet sources and fluorescent lamps for publicity lighting. Experimental diagnostics of the column plasma includes measurements of the axial electric field strength and of the axis densities of the four lowest excited states of xenon. The electric field is determined from probe measurements. The particle densities are derived from the results of tunable diode laser absorption spectroscopy. Experimental investigations are assisted by a self-consistent analysis of the dc positive column plasma. A comparison between calculated and measured values of the axial electric field strength and the densities of excited xenon atoms is presented and discussed. The validated model is used for optimization of the discharge conditions by variation of the discharge current, gas pressure, and tube radius with respect to the radiation power and efficiency of the 147 nm resonance line of xenon. The discussion includes an analysis of the power budget of the column plasma. © 2004 American Institute of Physics. [DOI: 10.1063/1.1704866]

## I. INTRODUCTION

In the last decade the environmental aspect became one of the important requirements in the development of light sources. From this point of view, weakly ionized plasmas in rare-gas mixtures containing xenon are favorite candidates for sources of vacuum ultraviolet (VUV) radiation. In addition, discharges in xenon based mixtures advise a large operating temperature range and an instant light output after switching on. By use of photoluminescence of appropriate phosphors they can also be applied as sources of visible light. Discharges in pure xenon or in mixtures operating at higher pressures and at relatively small electrode distances, such as microcells<sup>1,2</sup> or dielectric barrier discharges,<sup>3</sup> are applied in plasma display panels<sup>4–7</sup> or for backlighting. Under these conditions, the xenon excimer radiation is the significant output. Contrary to this the low-pressure discharges produce mainly the atomic resonance radiation<sup>8–10</sup> and are proposed to design tube sources based on a very similar technology as for standard fluorescent lamps. One of the possible applications of such sources is publicity lighting.<sup>11</sup> However, more investigations are needed to find optimal discharge parameters and operating conditions of such light sources concerning their radiation efficiency and output as well as their stable operation and life-time. Detailed experimental and theoretical investigations of the positive column plasma of a glow discharge in a mixture of 2% xenon and 98% helium have been performed in the frame of the present work. The glow discharge is dc operated at total gas pressures in the range from 1.5 to 3.5 Torr and discharge currents from 10 to 100 mA. The measurements of the absolute densities of excited Xe metastable and resonance atoms are important for testing model predictions of these discharges.

Thus one of the objectives of this work is to apply a technique based on tunable diode laser absorption measurements, which provides data for the four lowest excited states  $1s_2 - 1s_5$  (Paschen notation) of xenon over an extended range of current and total gas pressure. The paper is organized as follows. In Sec. II the experimental apparatus and methods of investigations are presented. Section III gives an overview of the applied model. The results of measurements and calculations for the electric field strength and the densities of excited xenon atoms are compared in Sec. IV. The validated model is used for the study of the influence of variations of discharge current, gas pressure, and tube radius on the VUV radiation power and efficiency with respect to the electrical input into the column plasma. Results of the calculations are presented and discussed.

## II. EXPERIMENT

### A. Setup

The experimental arrangement used for the laser absorption measurements is shown in Fig. 1. The main components are the discharge tube, the electric power supply, the tunable diode laser system with the detector, and electronics for signal processing. In order to allow the laser beam to pass axially through the positive column an U-shaped discharge tube with plane windows on both ends of the horizontal section is used. The electrodes are mounted in the vertical sections. Thus discharge regions close to the electrodes do not interact with the laser beam. An absorption length of 26.7 cm results along the part of the positive column in the horizontal section, which has an inner diameter of 17.5 mm. Electron-emitting tungsten coiled-coil filaments pasted with a mixture of Ba–Sr–Ca oxide are used as electrodes. The cathode is separately heated with a dc current of 1.5 A to force sufficient thermoionic emission. Two tungsten probes of 50  $\mu\text{m}$

<sup>a)</sup>Electronic mail: uhl@inp-greifswald.de

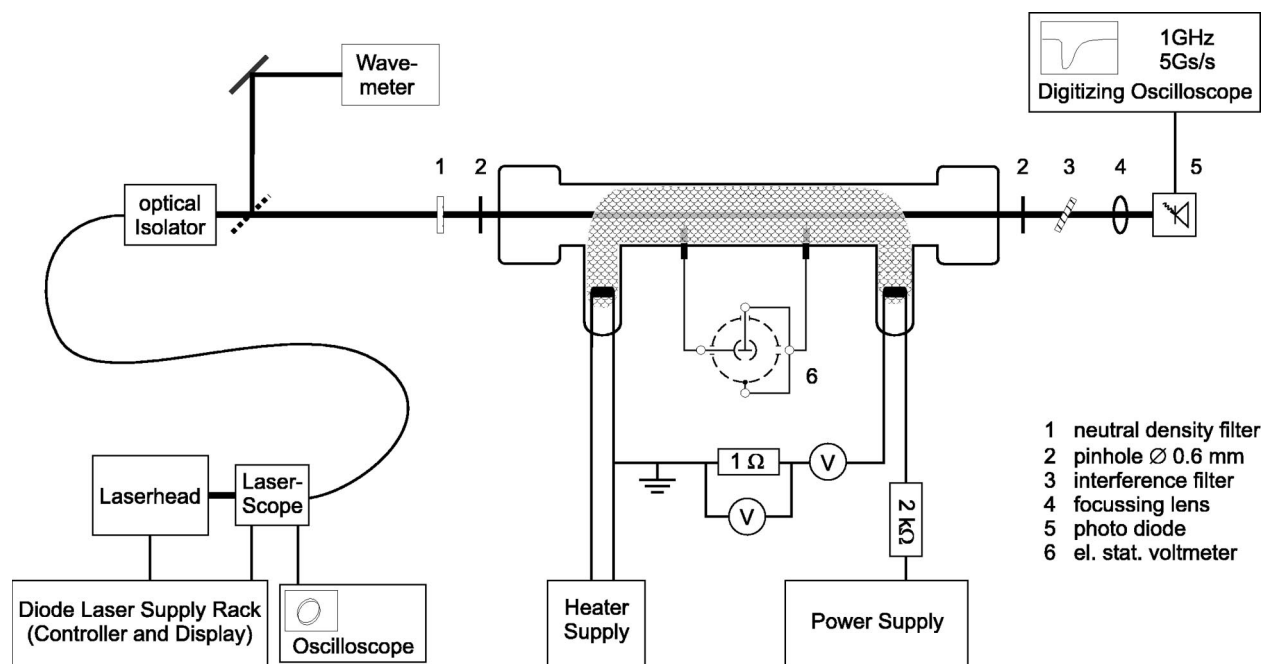


FIG. 1. Experimental setup for the investigation of the positive column plasma by laser atom absorption spectroscopy.

in diameter and 2 mm in length, encapsulated in glass sleeves of less than 1 mm in diameter are used to measure the difference of the floating potentials at their positions by means of a static voltmeter. The probes are positioned close to the tube axis in a distance of 10 cm. Considering this distance one obtains the axial electric field  $E_z$  in the positive column which, in addition, acts as a very sensitive indicator of the discharge stability. Already slight variations of  $E_z$  point to changes in the gas composition. The tube is mounted on a translation stage. By moving it perpendicular to the optical axis different radial positions of the positive column can be probed by the laser beam. The dc discharge is operated on a regulated power supply with a ballast resistor of 2 k $\Omega$  in series with the tube. The voltage across the discharge tube and the discharge current are measured by digital multimeters.

Before the experiment starts, the discharge tube has been baked out at temperatures of 380 °C for 8 h under high vacuum down to  $10^{-7}$  mbar. After this procedure the electrodes are processed at heating currents of about 1.5 A. Additional cleaning of the tube walls is achieved by several gas fillings with pure He and burn-ins at about 100 mA. The final state is reached after some fillings with a gas mixture of ultra pure He(99,999%) and Xe(99,99%). Then the tube is filled up to the desired pressure and sealed.

An external cavity diode laser (TUIOPTICS DL100) in Littrow-configuration is used as a background radiation source for the absorption measurements. The laser frequency has a typical bandwidth of a few megahertz and can be tuned over a range of about 40 GHz without mode-hopping by tilting the Littrow-Grating in front of the laser diode via a piezocrystal. The necessary signal (typically triangular

A servoloop inside the laser controller fits the diode injection current to the piezosignal in order to stabilize the adjusted laser mode.

Because of piezohysteresis effects the laser frequency does not exactly follow the control signal. The tuning behavior is monitored by the so-called LASERSCOPE from TUIOPTICS Corporation, Martinsried, Germany. Its main component is an etalon with small finesse. Two 90° phase-shifted sinusoidal signals are generated by the LASERSCOPE and can be displayed on an analog oscilloscope in XY-mode. Tuning the laser over a range that equals the free spectral range of the etalon causes a circle on the oscilloscope display. Mode-hops manifest itself in a reduced radius. Backreflections into the laser diode occur as little oscillations along the circular arc. In order to regulate the laser during a tuning cycle, the LASERSCOPE signal can be fed back into a servoloop.

At the output of the etalon the laser beam is coupled into a fiber optical waveguide which is connected to an optical isolator. The laser beam leaves the fiber having a Gaussian beam profile. Saturation of the observed optical transition is avoided by reducing the laser intensity via a neutral density filter within the optical path.

The radial resolution of the experiment is determined by two pinholes with diameters of 0.6 mm which are arranged directly in front of and behind the plane windows, respectively, of the discharge tube. An interference filter in front of the detector is used to reduce stray light from the discharge. The laser radiation which is transmitted through the plasma is detected by means of a photodiode Soliton UPD 500SP. To acquire the total transmitted laser intensity on the active diode area a short-focal-length lens focuses the laser beam

**B. Theoretical background of absorption measurements**

The net intensity balance of laser radiation at frequency  $\nu$  that passes a layer  $dx$  of a medium, is influenced by absorption and spontaneous as well as induced emission and given by the radiation transport equation

$$\frac{dI_\nu(x)}{dx} = -\kappa_\nu(x)I_\nu(x) + \varepsilon_{\nu,\text{ind}}(x)I_\nu(x) + \varepsilon_{\nu,\text{spont}}(x), \quad (1)$$

where  $\kappa_\nu(x)$  names the absorption coefficient and  $\varepsilon_{\nu,\text{ind}}(x)$ ,  $\varepsilon_{\nu,\text{spont}}(x)$  denote the coefficients of induced and spontaneous emission. Induced emission can be avoided by setting the laser power well below the saturation intensity  $I_s(\nu)$  of the observed transition<sup>12</sup>

$$I_s(\nu) = \frac{2\sqrt{2}h\nu^3 A_{21}}{c^2} \quad (2)$$

with the transition probability  $A_{21}$  and the speed of light  $c$ . Under the given experimental conditions spontaneous emission is also negligible<sup>13</sup> and than the solution of Eq. (1) yields the Lambert–Beer’s-law

$$I_\nu(L) = I_\nu(0)e^{-\int_0^L \kappa_\nu(x)dx}, \quad (3)$$

which describes the decay of light intensity due to absorption within a medium of the length  $L$ . The exponent defines the optical depth  $\tau_\nu$ , hence

$$\tau_\nu = \int_0^L \kappa_\nu(x)dx = -\ln\left(\frac{I_\nu(L)}{I_\nu(0)}\right) \quad (4)$$

is obtained. The absorption coefficient itself can be written as

$$\kappa_\nu(x) = \sigma_\nu N_\nu(x). \quad (5)$$

Here,  $N_\nu(x)$  is the particle number density of the lower energetic level, that is probed by the laser and

$$\sigma_\nu = \frac{e^2}{4\varepsilon_0 m_e c} f_{ik} P_\nu \quad (6)$$

is the photoabsorption cross-section, where  $e$  denotes the elementary charge,  $\varepsilon_0$  the permittivity,  $f_{ik}$  the oscillator strength of the observed transition, and  $P_\nu$  the line profile of the transition normalized according to  $\int_\nu P_\nu d\nu = 1$ .

Using Eq. (5) and assuming homogeneous distributed absorbing species gives an expression for the particle number density

$$N_\nu = \frac{4\varepsilon_0 m_e c}{e^2 f_{ik}} \frac{\tau_\nu}{P_\nu L} \equiv -\frac{4\varepsilon_0 m_e c^2}{e^2 f_{ik} P_\nu L} \ln\left(\frac{i(\lambda)}{i_0(\lambda)}\right), \quad (7)$$

where  $P_\lambda = P_\nu c/\lambda^2$ ,  $i(\lambda) \equiv I_\nu(L)$  and  $i_0(\lambda) \equiv I_\nu(0)$ .

**C. Measurement of particle number densities**

In the frame of the experimental work the four lowest excited states  $1s_2 - 1s_5$  of xenon are probed by laser radiation. Therefore, the laser is tuned to the optical transitions

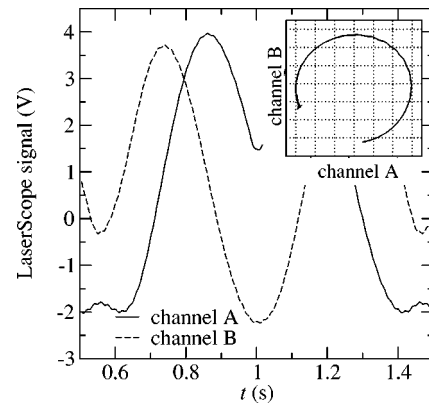


FIG. 2. Typical LaserScope signals; main frame: channels in  $y(t)$  mode with  $90^\circ$  phase shift, inset: same signals in  $xy$  mode. The laser is tuned over  $0.8 \times \text{FSR}$  of the etalon.

The determination of particle number densities of excited xenon states by laser absorption spectroscopy requires two series of measurements. The first one is done in order to analyze  $I_\nu(0)$  in dependence on the laser frequency in absence of absorbing species (plasma switched off). Herewith transmission properties of every optical component within the laser beam path are registered and the power modulation of the laser during scanning is considered. In the following the plasma is switched on and the actual absorption measurement is performed. Simultaneously with the laser intensity the LASERSCOPE signals are recorded in both series of measurements. The latter are used to realize a time correlation between the course of the laser intensity and the current laser frequency or its wavelength, respectively. The procedure is pointed out in the following.

The exact determination of the actual laser wavelength is fundamental in the scope of absorption experiments. A commercially available tool for this task is a Wavemeter (Burlleigh WA-4500, see Fig. 1) yielding absolute values with a limited temporal resolution of 0.1 s. Therefore, this device is used only for calibration. However, the LASERSCOPE can be applied for measuring relative laser frequency changes with the required temporal resolution of 0.2 ms during laser tuning. The free spectral range (FSR) of the LASERSCOPE etalon is determined once with the help of the Wavemeter. An example of typical LASERSCOPE signals is given in Fig. 2. The transfer function of the etalon is sinusoidal shaped. Displaying both LASERSCOPE channels on an oscilloscope in  $xy$  mode results in a full circle if the laser is tuned over the FSR of the etalon. The value of the phase angle on this circle is a measure for the relative frequency shift. In practice, this measurement is done by analyzing the phase angle with the help of a LABVIEW™ program,<sup>14</sup> that fits an analytic function to the measured circle. Finally the program assigns the calculated  $\Delta\lambda$  scale to the measured photodetector signals in every point in time (see Fig. 3).

Typically two tuning cycles of the laser are recorded for one absorption measurement. This allows an averaging over four absorption profiles in the following data analysis. At

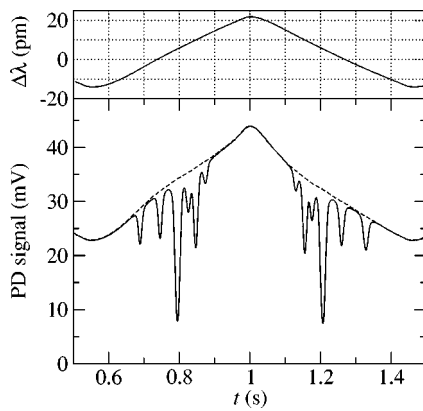


FIG. 3. Wavelength scaling of absorption signals; relative wavelength shift  $\Delta\lambda$  from the LaserScope signal in the upper frame and photodetector signals of the laser intensity with (solid line) and without plasma (dashed line) in the lower frame in dependence on time  $t$  during laser tuning.

function  $P(\lambda)$  as shown in Fig. 4 is obtained. The shape of a line profile function is mainly determined by the gas pressure of the tube filling. Hence for determining particle number densities at different discharge currents a reference line profile function is used, which has to be measured at a fixed discharge current whenever a new gas pressure is to be investigated.

### III. DESCRIPTION OF THE MODEL

A detailed self-consistent model of the cylindrical positive column of the xenon-helium dc discharge is used to assist in understanding the processes taking place in the plasma and in optimization of the VUV radiation output. The positive column is assumed to be axially symmetric and free of striations or other inhomogeneities, so that the plasma quantities can be supposed to be invariant to translations along the discharge axis and time independent. The model includes a self-consistent treatment of the space-charge field, the excited atom balances and the electron kinetics resolved in the radial space dimension. The cylindrical dc column plasma is described by a stationary hybrid method<sup>15</sup> which comprises the coupled solution of the space-dependent kinetic equation of electrons, the fluid equations of electrons, ions, and excited atoms, the Poisson equation for the radial space-charge

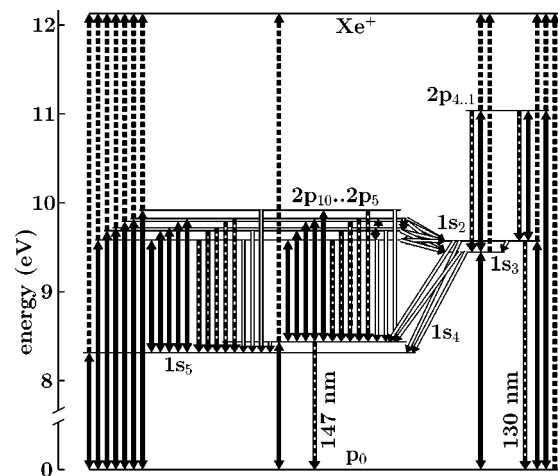
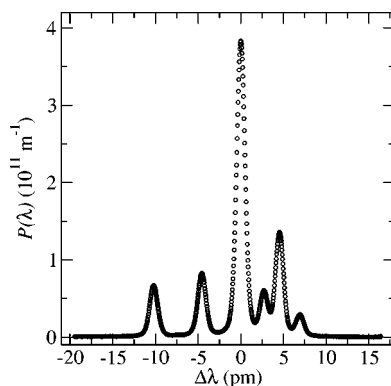


FIG. 5. Xenon energy level scheme and processes considered in the model: excitation and deexcitation in electron collisions (solid arrows), ionization in electron collisions (dashed arrows), radiative transitions (dashed double line arrows), and quenching processes (double line arrows) with xenon and helium ground state atoms.

potential, and the balance equation of the electron surface charge density at the tube wall. In particular, the radial space-charge potential as well as the electron production due to the ionization of ground-state and excited atoms are taken into account in the electron kinetic equation, which is solved applying the two-term approximation<sup>10,16</sup> of the velocity distribution function. The electron kinetic treatment yields radially dependent transport coefficients and mean frequencies of the ionization and excitation in electron collisions which are used to solve the fluid equations. The iterative coupling of the electron kinetic treatment and the solution of the fluid-Poisson equation system leads to a sufficiently accurate description of the space-charge confinement in the column plasma. The axial electric field is finally determined by a coupled treatment of the charge-carrier budget in the plasma volume and the plasma-wall interactions.<sup>17</sup>

The basic equations and details of the solution method have been already described in previous papers,<sup>15,16</sup> where the positive column plasma of a neon dc discharge has been studied. Specific aspects of the model to describe the collision and radiation processes and to treat the balances of the excited species in the considered helium-xenon mixture are given in Ref. 18.

However, an extension of the reaction kinetic model, which determines the densities of the most populated excited states in the helium-xenon column plasma and which is described in detail in Ref. 18 has been applied. The present model distinguishes 13 states of xenon: the ground state  $Xe(1p_0)$ , nine individual excited states, i.e., the metastable levels  $Xe(1s_5)$  and  $Xe(1s_3)$ , the resonant levels  $Xe(1s_4)$  and  $Xe(1s_2)$ , five lowest  $p$ -levels  $Xe(2p_{10})$ ,  $Xe(2p_9)$ ,  $Xe(2p_8)$ ,  $Xe(2p_7)$ ,  $Xe(2p_6)$ , two lumped states  $Xe(2p_5 + 3d + 3s, \dots, 9s)$  [denoted further for brevity reasons as  $Xe(2p_5)$ ] and  $Xe(2p_{4,\dots,1})$ , and the ion  $Xe^+$  in the ground state. Because of the high values of excitation thresholds of helium atoms a simplified level model of helium has been

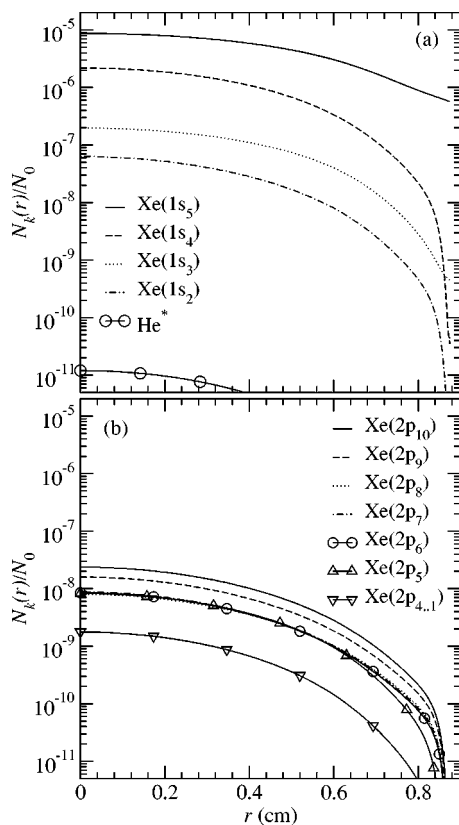


FIG. 6. Radial variation of the densities  $N_k$  of excited xenon and helium atoms for  $I_z=60$  mA,  $p_0=2.5$  Torr, and  $r_w=0.87$  cm.

the xenon level scheme and the manifold of the processes included in the model. The reaction kinetic model takes into account over 190 plasma-chemical processes, including exciting, deexciting, and ionizing electron-heavy particle collisions, chemoionization, radiation, quenching, and formation of excimer molecules. The choice and the sources of the atomic data, rate constants, radiation life-times, as well as the description of the equation systems for the determination of densities of heavy particles and their radial variation are presented in Ref. 18.

The reaction kinetic model given in Ref. 18 has been extended by the individual treatment of the levels  $Xe(2p_9), \dots, Xe(2p_5)$  to improve the accuracy of the description of the  $s$ -levels. This has been done because the  $Xe(1s_5)$  and  $Xe(1s_4)$  states are closely coupled with these  $p$ -levels due to excitation processes in electron collisions and spontaneous emission processes in the singlet system. In addition, quenching processes between these  $p$ -levels and the  $Xe(1s_3)$  and  $Xe(1s_2)$  states are important for the establishment of the densities in the triplet system.<sup>18</sup>

Additional data for the treatment of the individual  $p$ -levels have been taken also from the sources given in Ref. 18, i.e., cross sections of Nakazaki<sup>19</sup> are used to describe the excitation of the  $p$ -levels from the ground state in electron collisions, stepwise excitation cross sections are calculated according to Vriens and Smeets,<sup>20</sup> Deutsch-Märk formalism<sup>21</sup> is used to determine stepwise ionization cross

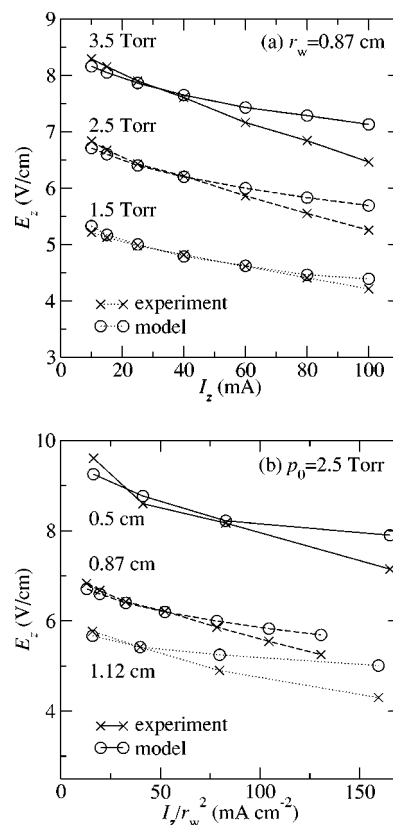


FIG. 7. Experimental data (crosses) and data predicted by the model (circles) for the axial electric field strength  $E_z$  as a function of the discharge current  $I_z$  for three different gas pressures  $p_0$  and a tube radius  $r_w=0.87$  cm (a) and for three different tube radii in the case of  $p_0=2.5$  Torr (b).

densities of excited xenon atoms for the case of a gas pressure of 2.5 Torr, a tube radius of 0.87 cm, and a discharge current of 60 mA. The metastable  $Xe(1s_5)$  state is by far the most occupied excited level. Its density in the axis is by a factor of  $10^5$  smaller than the helium buffer gas density and, hence, by a factor of  $10^3$  smaller than the xenon ground state density under the considered conditions. Because of the pronounced radial space charge confinement of the plasma all excited atom densities decrease from their axis value by more than one order of magnitude over the column cross section.<sup>18</sup> The density of helium metastable atoms is by about six orders of magnitude smaller than the  $Xe(1s_5)$  density. Hence, processes of excited helium atoms are of negligible importance in the reaction kinetics as well as in the charge carrier budget under the considered conditions.

#### IV. RESULTS AND DISCUSSION

##### A. Experimental results and validation of the model

A detailed comparison between the model calculations and the measurements has been performed for the axial electric field strength and for the axis densities of xenon atoms in four lowest excited states (i.e.,  $1s_5$ ,  $1s_4$ ,  $1s_3$ , and  $1s_2$ ) in the column plasma.

Figure 7 presents measured and calculated values of the

# Explore Litigation Insights

Docket Alarm provides insights to develop a more informed litigation strategy and the peace of mind of knowing you're on top of things.

## Real-Time Litigation Alerts



Keep your litigation team up-to-date with **real-time alerts** and advanced team management tools built for the enterprise, all while greatly reducing PACER spend.

Our comprehensive service means we can handle Federal, State, and Administrative courts across the country.

## Advanced Docket Research



With over 230 million records, Docket Alarm's cloud-native docket research platform finds what other services can't. Coverage includes Federal, State, plus PTAB, TTAB, ITC and NLRB decisions, all in one place.

Identify arguments that have been successful in the past with full text, pinpoint searching. Link to case law cited within any court document via Fastcase.

## Analytics At Your Fingertips



Learn what happened the last time a particular judge, opposing counsel or company faced cases similar to yours.

Advanced out-of-the-box PTAB and TTAB analytics are always at your fingertips.

## API

Docket Alarm offers a powerful API (application programming interface) to developers that want to integrate case filings into their apps.

## LAW FIRMS

Build custom dashboards for your attorneys and clients with live data direct from the court.

Automate many repetitive legal tasks like conflict checks, document management, and marketing.

## FINANCIAL INSTITUTIONS

Litigation and bankruptcy checks for companies and debtors.

## E-DISCOVERY AND LEGAL VENDORS

Sync your system to PACER to automate legal marketing.